

Möbius-topological auxiliary function for f electrons

Biaoyan Hu^{1,2,*}

¹Quantum Science Center of Guangdong-Hong Kong-Macao Greater Bay Area, Shenzhen 518045, China

²Department of Physics, Southern University of Science and Technology, Shenzhen 518055, China

f -electron systems exhibit a subtle interplay between strong spin-orbit coupling and crystal-field effects, producing complex energy landscapes that are somewhat cumbersome to compute. We introduce auxiliary functions, constructed by extending hydrogen-like wave functions through a modification of the Legendre function. These functions often possess a Möbius-like topology, satisfying $\psi(\varphi) = -\psi(\varphi + 2\pi)$, while their squared modulus respects inversion symmetry. By aligning $|\psi|^2$ with the symmetry of the crystal field, they allow rapid determination of eigenstate structures without the need for elaborate calculations. The agreement with established results indicates that these functions capture the essential physics while offering considerable computational simplification.

Introduction.— Understanding electronic eigenstates in solids is essential for interpreting their magnetic, spectroscopic, and thermodynamic properties. An early quantum-mechanical treatment of atomic term splitting in crystals was provided by Bethe [1], who analyzed how crystalline electric fields lift electronic degeneracies. This laid the foundation for crystal field theory developed by Van Vleck [2], providing a general framework applied to magnetic and spectroscopic phenomena. Since then, crystal field theory has guided the interpretation of spectra and thermodynamic behavior in minerals with transition metals [3], and clarified structure-property relations in luminescent materials [4]. More recently, crystal-field analysis has become a key tool for probing rare-earth magnetism and correlated f -electron systems [5–11].

Formal links between quantum operators and classical multipoles have been established [12]. In particular, the crystal-field Hamiltonian can be expressed via the Stevens operator method [13] as $H_{\text{CF}} = \sum_{l,m} B_l^m O_l^m$, where B_l^m and O_l^m are the crystal-field parameters and Stevens operators, respectively [14].

Existing methods for f -electron systems are fully capable but often cumbersome due to proliferating notations and intricate derivations. A more direct approach yielding explicit eigenstate structures would greatly simplify analysis of these technically demanding systems.

Auxiliary function.— Motivated by the need for a simpler approach, we introduce a modified theoretical framework based on the hydrogen-like Schrödinger equation. By modifying the Legendre function, we construct functions for all angular momenta, including half-integer values, enabling direct determination of f -electron eigenstate structures.

The Schrödinger equation for an electron under Coulomb potential in Gaussian units is given by:

$$\left(-\frac{\hbar^2}{2m_e}\nabla^2 - \frac{Ze^2}{r}\right)\psi(r, \theta, \varphi) = E\psi(r, \theta, \varphi), \quad (1)$$

where m_e is the electron mass and ∇^2 is the Laplacian operator. This equation is generally applicable only to hydrogen-like atoms, but with Slater's rules [15], it can be

approximately applied to multi-electron systems. However, for f electrons with strong spin-orbit coupling, the equation cannot yield correct wave functions. In this work, fully aware of its limitations, we nonetheless apply it to f electrons.

The solution of Eq. 1 can be expressed as follows:

$$\psi(r, \theta, \varphi) = R(r)Y_l^m(\theta, \varphi) \propto R(r)P_l^m(\cos\theta)e^{im\varphi},$$

where $Y_l^m(\theta, \varphi)$ are spherical harmonics constructed from the associated Legendre polynomials $P_l^m(\cos\theta)$. Here, l and m denote the degree and order of P_l^m , corresponding to the orbital angular momentum and its z -component. Throughout this paper, unless otherwise stated, $l \in \mathbb{N}$ and $m \in \mathbb{Z}$ satisfy $-l \leq m \leq l$.

The f electrons experience strong spin-orbit coupling, with total angular momentum given by $\mathbf{J} = \mathbf{L} + \mathbf{S}$. Consequently, the solutions of Eq. 1 should be expressed in terms of the total angular momentum J and its projection along the z -axis, M . This leads to a new function:

$$\begin{aligned} \psi(r, \theta, \varphi) &\equiv R(r)Y_J^M(\theta, \varphi) \\ &\equiv R(r)\sqrt{\frac{(2J+1)(J-M)!}{4\pi(J+M)!}}P_J^M(\cos\theta)e^{iM\varphi}, \end{aligned} \quad (2)$$

where $2J \in \mathbb{N}$ and $M \in \{-J, -J+1, \dots, J\}$; the same conventions apply throughout. Here, the factorial is defined by $x! \equiv \Gamma(x+1)$, and this convention is used consistently below. We refer to the function in Eq. 2 as the *auxiliary function*.

The auxiliary function is not the true wave function of an f electron, but a simplified form that captures many essential features of the actual wave function. Both share the same symmetries, and the integrals of their squared moduli are equal to one. The difference lies in continuity. While the wave function and its squared modulus are continuous, the auxiliary function becomes discontinuous when J is a half-integer. For superposed states, the auxiliary function's squared modulus is sometimes discontinuous on the equatorial plane. Despite this, the auxiliary function is useful, as it circumvents the often

cumbersome computation and allows one, through relatively simple analysis, to directly obtain the eigenstate structures of f electrons under a crystal field.

The squared modulus of the auxiliary function is referred to as the *auxiliary density*. For f electrons, its symmetry matches that of the crystal field, allowing one to infer the eigenstate structures directly from the crystal field symmetry.

The P_J^M in Eq. 2 is an extension of P_l^m , and there exist multiple ways to generalize P_l^m . Legendre functions with non-integer degrees and orders have been discussed extensively [16–31]. The most widely used form involves hypergeometric functions [17–28] and was initially introduced by Hobson [20], though this origin is often overlooked. Some works explicitly refer to these as *Hobson’s associated Legendre functions* [22]. For convenience, this paper refers to them as *Hobson’s Legendre functions*.

For half-integer degrees and orders (as opposed to arbitrary fractional values), the generalized Rodrigues formula (Supplemental Material (SM) Eq. S21) can be used to compute $P_J^M(x)$ [16]. Since $J+M$ is a natural number, the derivative of order $J+M$ is well defined. We find that this procedure yields results identical to Hobson’s Legendre functions, and thus we treat them as belonging to the same class, without discussing them separately.

Hunter *et al.* proposed an alternative solution [29, 30], identifying regularities of factors for integer orders and degrees and generalizing them to half-integer cases. The resulting expressions satisfy the associated Legendre equation, and a table of factors was provided. We refer to these as *Hunter’s Legendre functions*.

Although tables are inherently limited, once such patterns are established, a general formula can, in princi-

ple, be written and extended to arbitrary parameters. Closed-form expressions of this kind have been presented previously [31–33], with Bildstein in particular generalizing the associated Legendre polynomials to half-integer degrees and orders [31]. Both approaches ultimately lead to the same system, differing only in coefficients. We therefore treat Bildstein’s results as equivalent to those of Hunter *et al.*

Current Legendre functions can be broadly classified into two types: Hobson’s and Hunter’s, both of which satisfy the associated Legendre equation. To construct a useful auxiliary function that resembles a wave function, the Legendre function must not only satisfy the associated Legendre equation but also three additional key properties. Initially, it should be square-integrable, allowing normalization. Next, functions of opposite orders should exhibit similarity, so that auxiliary densities corresponding to opposite angular momenta share the same overall shape. Finally, Legendre functions’ parity must match that of $J+M$. This guarantees that the auxiliary density of the superposed states preserves inversion symmetry, a feature central to our work.

Associated Legendre polynomials of integer degree and order elegantly satisfy all these properties. However, for half-integer degrees and orders, the properties become mutually exclusive to some extent. As shown in Tab. I, neither Hobson’s nor Hunter’s Legendre functions can simultaneously satisfy all these requirements. Our analysis shows that introducing the sign function $\text{sgn}(x)$ resolves this conflict.

The Legendre function in this work is defined from Hobson’s Legendre function as follows:

$$P_J^M(x)_{\text{this work}} \equiv (-1)^{(M+|M|)[\frac{1}{2}+2J+J\text{sgn}(x)]} \frac{(J+M)!}{(J-|M|)!} P_J^{-|M|}(x)_{\text{Hobson}} \quad (3)$$

$$= (-1)^{(M+|M|)[\frac{1}{2}+2J+J\text{sgn}(x)]} \frac{(J+M)!}{(J+|M|)!} \frac{(1-x^2)^{\frac{|M|}{2}}}{2^J} \sum_{k=0}^{\lfloor \frac{J-|M|}{2} \rfloor} \frac{(-1)^k (2J-2k)!}{k! (J-k)!} \frac{x^{J-|M|-2k}}{(J-|M|-2k)!}. \quad (4)$$

An example is shown in Fig. 1. For $J = 5/2$ and $M = 3/2$, neither Hobson’s nor Hunter’s Legendre functions satisfy all four properties. In contrast, our function avoids the divergence present in Hobson’s form while preserving the correct parity that Hunter’s function lacks. Although it is singular at $x = 0$, this feature is necessary to satisfy all core requirements.

When J and M are half-integers, the wave function $\psi \propto P_J^M(\cos\theta)e^{iM\varphi}$ becomes antiperiodic in φ , satisfying $\psi(r, \theta, \varphi) = -\psi(r, \theta, \varphi + 2\pi)$ and thereby exhibiting a Möbius-type topology, as illustrated in Fig. 2a. To

maintain single-valuedness, continuity of the auxiliary function with respect to φ must be relinquished. For instance, if φ is defined on $[0, 2\pi)$, the auxiliary function is necessarily discontinuous at $\varphi = 0$. Nevertheless, the density $|\psi|^2$ remains fully periodic and continuous in φ .

Hunter *et al.* similarly mentioned the Möbius band when discussing half-integer spherical harmonics [29], as it arises from the $e^{iM\varphi}$ term for half-integer M . The difference lies in their Legendre function, whose parity does not meet the requirements of this work.

This auxiliary function approach provides an efficient

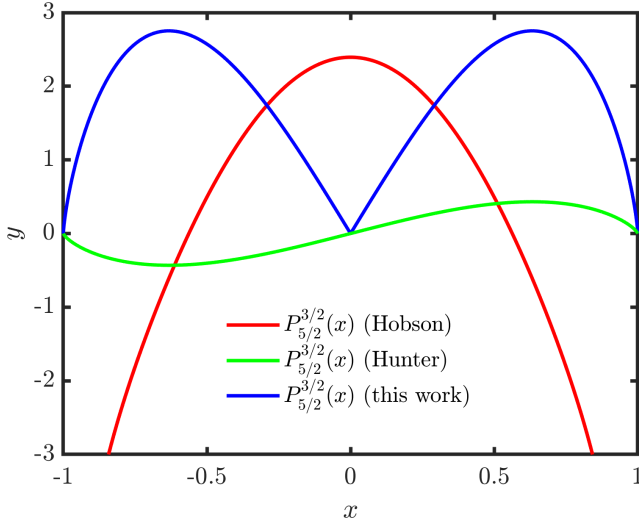


FIG. 1. Comparison of $P_{5/2}^{3/2}(x)$ from Hobson [20, 21], Hunter *et al.* [29, 30], and the present work. Hobson's $P_{5/2}^{3/2}(x) = (8x^4 - 12x^2 + 3)/\sqrt{\frac{\pi}{2}\sqrt{(1-x^2)^3}}$ is an even function that diverges as $x \rightarrow \pm 1$, with a squared modulus that is non-integrable. Hunter's $P_{5/2}^{3/2}(x) = x(1-x^2)^{3/4}$ is an odd function and integrable. In contrast, as presented here in this work, $P_{5/2}^{3/2}(x) = 8|x|\sqrt{2/\pi}(1-x^2)^{3/4}$ is an even function that is integrable.

TABLE I. Comparison of $P_J^M(x)$ for $x \neq 0$ as defined by Hobson [20, 21], Hunter *et al.* [29, 30], and in this work. The symbols \checkmark and \times denote whether the condition is always satisfied or not, respectively.

Property of $P_J^M(x)$	Hobson	Hunter	This work
Associated Legendre equation	\checkmark	\checkmark	\checkmark
$\int_{-1}^1 P_J^M(x) ^2 dx < \infty$	\times	\checkmark	\checkmark
$\frac{\partial}{\partial x} \left \frac{P_J^{-M}(x)}{P_J^M(x)} \right = 0$	\times	\checkmark	\checkmark
$P_J^M(-x) = (-1)^{J+M} P_J^M(x)$	\checkmark	\times	\checkmark

and accurate tool for predicting f -electron eigenstates in crystal fields. An auxiliary density consistent with the local symmetry is constructed, allowing the eigenstate structures to be determined without exhaustive diagonalization. Predictions based on this framework show excellent agreement with full numerical solutions, offering both computational efficiency and insight into the electronic structure of strongly correlated f electrons.

Symmetry analysis.— Auxiliary functions can be employed to determine energy eigenstates, provided their densities conform to the crystal-field symmetry. The eigenstate structure is dictated by rotational symmetry together with a horizontal mirror plane, while vertical mirror planes constrain the phases of the complex coefficients forming the eigenstate components.

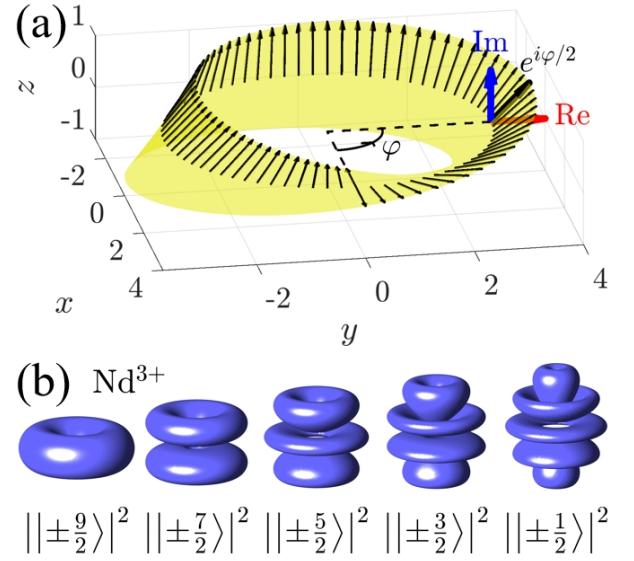


FIG. 2. (a) The factor $e^{i\varphi/2}$ is plotted along a circular arc of radius 3, with its vector trajectory forming a Möbius strip. (b) Auxiliary densities distribution of f -electron states in Nd^{3+} ($J = 9/2$). Kets $|M\rangle$ denote the quantum states. The auxiliary densities exhibit $O(2)$ symmetry, and the surface encloses 50% of the total density.

The auxiliary density of a pure eigenstate with a single M exhibits continuous $O(2)$ rotational symmetry. A superposition, however, generally breaks this symmetry, reducing it to discrete rotational symmetries. For instance, for a two-state superposition $|\psi\rangle = C_1 |M_1\rangle + C_2 |M_2\rangle$, the auxiliary density is:

$$\begin{aligned}
 |\psi|^2 &= |C_1 |M_1\rangle + C_2 |M_2\rangle|^2 \\
 &= |A(r, \theta)e^{iM_1\varphi} + B(r, \theta)e^{iM_2\varphi}|^2 \\
 &= (Ae^{iM_1\varphi} + Be^{iM_2\varphi})(A^*e^{-iM_1\varphi} + B^*e^{-iM_2\varphi}) \\
 &= |A|^2 + |B|^2 + 2|AB|\cos[(M_1 - M_2)\varphi + \arg(AB^*)],
 \end{aligned}$$

where A and B are independent of φ . The auxiliary density thus has $|M_1 - M_2|$ -fold rotational symmetry. For example, $|M_1 - M_2| = 3$ gives threefold symmetry; $= 2$, twofold; $= 1$, no rotational symmetry.

For a general superposition of N states that $|\psi\rangle = \sum_{j=1}^N A_j(r, \theta)e^{iM_j\varphi}$, the auxiliary density is:

$$\begin{aligned}
 |\psi|^2 &= \left| \sum_{j=1}^N A_j(r, \theta)e^{iM_j\varphi} \right|^2 \\
 &= \sum_{j=1}^N |A_j|^2 + \sum_{j \neq k} |A_j A_k| \cos[(M_j - M_k)\varphi + \arg(A_j A_k^*)].
 \end{aligned} \tag{5}$$

Therefore, the auxiliary density exhibits κ -fold rotational symmetry if and only if the following condition hold:

$$\kappa = \text{gcd}(M_j - M_k), \tag{6}$$

where gcd (greatest common divisor) is taken over all pairs (j, k) . The corresponding eigenstate, with $|\psi|^2$ exhibiting κ -fold rotational symmetry, takes the form:

$$|\psi\rangle = \sum_{j=0}^{\lfloor \frac{2J-q}{\kappa} \rfloor} C_j |J - \kappa j - q\rangle, \quad q \in \{0, 1, \dots, \kappa - 1\}. \quad (7)$$

The auxiliary density is always inversion-symmetric (see proof in SM). When combined with even-fold rotational symmetry, it automatically exhibits horizontal mirror symmetry. For odd-fold rotational symmetry that possesses inherent inversion symmetry, an introduction of a horizontal mirror plane will double the rotational symmetry, effectively making it even-fold. In this sense, horizontal mirror symmetry amplifies odd-fold rotations while leaving even-fold rotations unchanged. Depending on κ , this enhancement changes the symmetry from C_κ to either $C_{2\kappa m}$ or $C_{\kappa m}$ as:

$$I + C_\kappa = \begin{cases} S_{2\kappa} \xrightarrow{+\sigma_z} C_{2\kappa m}, & \text{if } \kappa \text{ is odd,} \\ C_{\kappa m} \xrightarrow{+\sigma_z} C_{\kappa m}, & \text{if } \kappa \text{ is even.} \end{cases} \quad (8)$$

Rotational and horizontal mirror symmetries constrain the composition of an eigenstate but not its absolute orientation in φ , which is fixed by vertical mirror symmetry. From Eq. 5, the phase differences $\text{Arg}(A_j A_k^*)$ determine the azimuthal positions of the density maxima. For a two-component state $|\psi\rangle = C_1|M_1\rangle + C_2|M_2\rangle$, vertical mirror symmetry at $\varphi = \varphi_m$ imposes:

$$\tan \text{Arg} \frac{C_2}{C_1} = \tan[(M_1 - M_2)\varphi_m], \quad (9)$$

where the tangent removes the ambiguity of a global phase. While the extension to multi-component states is more involved, this relation illustrates how auxiliary functions accommodate vertical mirror symmetry.

The above laws regarding the eigenstates can also be obtained using the crystal field Hamiltonian in Stevens-operator form. However, the auxiliary function provides a simpler and conceptually novel perspective.

Example.— We consider the optically active material NdCl_3 [34] as an example. The Nd^{3+} ion ($J = 9/2$) experiences a crystal field generated by the nine surrounding Cl^- ions. First, this environment exhibits a threefold rotational symmetry, yielding $\text{gcd}(M_j - M_k) = 3$. Second, the presence of a horizontal mirror plane leads to $I + C_3 = S_6 \xrightarrow{+\sigma_z} C_6$, so that the auxiliary function acquires six-fold rotational symmetry with $\text{gcd}(M_j - M_k) = 6$. As a result, the eigenstates take the forms:

$$C_{\pm\frac{9}{2}}|\pm\frac{9}{2}\rangle + C_{\mp\frac{3}{2}}|\mp\frac{3}{2}\rangle, \quad C_{\pm\frac{7}{2}}|\pm\frac{7}{2}\rangle + C_{\mp\frac{5}{2}}|\mp\frac{5}{2}\rangle, \quad |\pm\frac{1}{2}\rangle.$$

Third, taking into account the vertical mirror plane at $\varphi_m = -6.72^\circ$, Eq. 9 gives:

$$\tan \text{Arg} \left(C_{\pm\frac{9}{2}} / C_{\mp\frac{3}{2}} \right) = \tan \text{Arg} \left(C_{\pm\frac{7}{2}} / C_{\mp\frac{5}{2}} \right) \approx \pm 0.849.$$

These relations, derived from the auxiliary functions, are confirmed by McPhase simulations [35], which produce eigenstates consistent with the forms above. The extracted phase ratios,

$$\tan \text{Arg} \left(C_{\pm\frac{9}{2}} / C_{\mp\frac{3}{2}} \right) \approx \tan \text{Arg} \left(C_{\pm\frac{7}{2}} / C_{\mp\frac{5}{2}} \right) \approx \pm 0.824,$$

show excellent agreement with the predicted values. The auxiliary densities fully preserve the crystal-field symmetry, further validating the method. See Supplementary Materials for details.

Discussion.— In the presence of degeneracy, certain eigenstates may appear to deviate from the predicted pattern of the auxiliary functions, as they can form linear combinations within the degenerate subspace. A suitable basis transformation restores the expected form, as illustrated in NdCl_3 , where the degenerate $|\pm\frac{1}{2}\rangle$ states may combine into $\frac{1}{\sqrt{2}}(|+\frac{1}{2}\rangle + |-\frac{1}{2}\rangle)$, but agreement with the rules is recovered in the proper basis.

The factor $\text{sgn}(x)$ ensures the correct parity of half-integer M states and preserves inversion symmetry in the auxiliary density. Its use, however, sometimes leads to discontinuities at the equatorial plane ($\theta = 90^\circ$) for superpositions with odd rotational symmetry, as in the state $\frac{1}{\sqrt{2}}(|+\frac{1}{2}\rangle + |-\frac{1}{2}\rangle)$. The specific form of $\text{sgn}(x)$ is not unique; any factor that enforces the correct parity for positive half-integer M suffices. The expression $[\frac{1}{2} + 2J + J, \text{sgn}(x)]$ in Eqs. (3) and (4) could be reduced to $[\frac{1}{2} + \text{sgn}(x)]$, but we retain the original form to ensure that the Legendre function's sign near $x = 0$ matches Hobson's.

Since spin S and orbital angular momentum L are neglected, the auxiliary functions provide only approximate descriptions of f -electron wave functions. It does not apply to cases such as Gd^{3+} , where $L = 0$ and the ion forms singlets despite the theory predicting multi-component states.

Nevertheless, the auxiliary functions offer a practical tool: small discontinuities or deviations in degenerate systems do not diminish its utility for symmetry analysis and qualitative characterization of eigenstate structures.

Conclusion and Outlook.— By extending Legendre functions to half-integer degrees and orders, we construct auxiliary functions with Möbius-like topologies. These functions provide an efficient framework for predicting eigenstates in f -electron systems. They naturally respect crystal-field symmetries, including multi-fold rotational and mirror symmetries, and offer an intuitive approach for determining eigenstate configurations. Compared with full crystal-field calculations, the auxiliary functions reproduce eigenstate structures with high accuracy, demonstrating their practical value for analyzing complex f -electron materials.

The predictive success of these auxiliary functions suggests they capture essential physical principles underlying f -electron eigenstates. While their full physical sig-

nificance remains to be elucidated, this approach opens promising avenues for further exploration, including applications to other strongly correlated or geometrically frustrated systems, investigations of deeper connections with symmetry and topology, and interpretation of experimental observations in complex materials.

Acknowledgment.— The author gratefully acknowledges Hanteng Wang for valuable discussions and suggestions. The author also thanks colleagues from Southern University of Science and Technology for their assistance with the use of McPhase.

* hubiaoyan@quantumsc.cn

- [1] H. Bethe, *Termaufspaltung in kristallen*, *Annalen der Physik* **395**, 133 (1929).
- [2] J. H. V. Vleck, *The Theory of Electric and Magnetic Susceptibilities* (Oxford University Press, 1932).
- [3] R. G. Burns, *Mineralogical applications of crystal field theory* (Cambridge university press, 1993).
- [4] Z. Song and Q. Liu, Basic crystal field theory—a simple and useful tool to understand the structure–property relationship in luminescent materials, *Optical Materials: X* **16**, 100189 (2022).
- [5] N. Kabeya, S. Takahara, T. Arisumi, S. Kimura, K. Araki, K. Katoh, and A. Ochiai, Eigenstate analysis of the crystal electric field at low-symmetry sites: Application for an orthogonal site in the tetragonal crystal $\text{Ce}_2\text{Pd}_2\text{Pb}$, *Physical Review B* **105**, 014419 (2022).
- [6] D. Ueta, R. Kobayashi, H. Sawada, Y. Iwata, S.-i. Yano, S. Kuniyoshi, Y. Fujisawa, T. Masuda, Y. Okada, and S. Itoh, Anomalous magnetic moment direction under magnetic anisotropy originated from crystalline electric field in van der waals compounds CeTe_3 and CeTe_2Se , *Journal of the Physical Society of Japan* **91**, 094706 (2022).
- [7] O. P. Uzoh, S. Kim, and E. Mun, Influence of crystalline electric field on the magnetic properties of CeCd_3X_3 ($X = \text{P, As}$), *Physical Review Materials* **7**, 013402 (2023).
- [8] M. M. Bordelon, S. S. Fender, S. Thomas, J. D. Thompson, E. D. Bauer, and P. F. Rosa, Structural anomaly and crystalline electric field excitations in low-dimensional KU_2Te_6 , *Physical Review B* **108**, 064406 (2023).
- [9] D. Ram, L. Joshi, and Z. Hossain, Crystalline electric field and large anomalous hall effect in NdGaGe single crystals, *Journal of Magnetism and Magnetic Materials* **605**, 172326 (2024).
- [10] S. Guchhait, A. Painganoor, S. Islam, J. Sichelschmidt, M. Le, N. Christensen, and R. Nath, Magnetic and crystal electric field studies of the rare earth based square lattice antiferromagnet NdKNaNbO_5 , *Physical Review B* **110**, 144434 (2024).
- [11] S. Guchhait, R. Kolay, A. Magar, and R. Nath, Magnetic and crystal electric field studies of the Yb^{3+} -based triangular lattice antiferromagnets $\text{NaSrYb(BO}_3)_2$ and $\text{K}_3\text{YbSi}_2\text{O}_7$, *Physical Review B* **111**, 214437 (2025).
- [12] H. Kusunose, Description of multipole in f-electron systems, *Journal of the Physical Society of Japan* **77**, 064710 (2008).
- [13] K. W. H. Stevens *et al.*, Matrix elements and operator equivalents connected with the magnetic properties of rare earth ions, *Proceedings of the Physical Society. Section A* **65**, 209 (1952).
- [14] M. T. Hutchings, Point-charge calculations of energy levels of magnetic ions in crystalline electric fields, in *Solid state physics*, Vol. 16 (Elsevier, 1964) pp. 227–273.
- [15] J. C. Slater, Atomic shielding constants, *Physical Review* **36**, 57 (1930).
- [16] Z. Bak, Half-infinite quantum vortex sheets, *Philosophical Magazine Letters* **83**, 655 (2003).
- [17] N. N. Lebedev, R. A. Silverman, and D. B. Livhtenberg, *Special Functions and Their Applications* (Prentice-Hall, 1965).
- [18] C. Hwang and S.-K. Chen, Fully normalized spherical cap harmonics: Application to the analysis of sea-level data from TOPEX/POSEIDON and ERS-1, *Geophysical Journal International* **129**, 450 (1997).
- [19] R. L. Liboff, Conical quantum billiard revisited, *Quarterly of Applied Mathematics* **59**, 343 (2001).
- [20] E. W. Hobson, On a type of spherical harmonics of unrestricted degree, order, and argument, *Proceedings of the Royal Society of London* **59**, 189 (1896).
- [21] E. W. Hobson, *The theory of spherical and ellipsoidal harmonics* (CUP Archive, 1931).
- [22] E. T. Whittaker and G. N. Watson, *A Course of Modern Analysis: An Introduction to the General Theory of Infinite Processes and of Analytic Functions; with an Account of the Principal Transcendental Functions* (Cambridge University Press, Cambridge, 1915).
- [23] M. Abramowitz and I. A. Stegun, eds., *Handbook of Mathematical Functions with Formulas, Graphs, and Mathematical Tables*, National Bureau of Standards Applied Mathematics Series (US Government Printing Office, 1948).
- [24] H. Bateman and A. Erdélyi, *Higher transcendental functions, volume I* (McGraw-Hill Book Company, 1953).
- [25] N. O. Virchenko and I. Fedotova, *Generalized associated Legendre functions and their applications* (World Scientific, 2001).
- [26] R. S. Maier, Legendre functions of fractional degree: Transformations and evaluations, *Proceedings of the Royal Society A: Mathematical, Physical and Engineering Sciences* **472**, 20160097 (2016).
- [27] P. E. Creasey and A. Lang, Fast generation of isotropic gaussian random fields on the sphere, *Monte Carlo Methods and Applications* **24**, 1 (2018).
- [28] L. Durand, Fractional operators and multi-integral representations for associated legendre functions, *Journal of Mathematical Physics* **63**, 033503 (2022).
- [29] G. Hunter, P. Ecimovic, I. Schlifer, I. M. Walker, D. Beamish, S. Donev, M. Kowalski, S. Arslan, and S. Heck, Fermion quasi-spherical harmonics, *Journal of Physics A General Physics* **32**, 795 (1999).
- [30] G. Hunter and M. Emami-Razavi, Properties of fermion spherical harmonics, *arXiv preprint quant-ph/0507006* (2005).
- [31] S. Bildstein, Half theory fractional angular momentum and the application of fractional derivatives to quantum mechanics, *Journal of Mathematical Physics* **59** (2018).
- [32] D. W. Jepsen, E. F. Haugh, and J. O. Hirschfelder, The integral of the associated legendre function, *Proceedings of the National Academy of Sciences* **41**, 645 (1955).
- [33] J. An, Z. Wang, and Y. Du, Modeling regional ionosphere by adjusted spherical harmonic analysis, in *Global Navi-*

gation Satellite System: Technology Innovation and Application (Scientific Research Publishing (SciRes), 2009) pp. 138–143.

[34] M. Yin and J.-C. Krupa, Superfluorescence from NdCl₃,

Chemical physics letters **314**, 27 (1999).

[35] M. Rotter, Using mcphase to calculate magnetic phase diagrams of rare earth compounds, Journal of Magnetism and Magnetic Materials **272**, E481 (2004).

Supplemental Material for “Möbius-topological auxiliary function for f electrons”

RADIAL FACTOR OF THE AUXILIARY FUNCTION

In this work, the auxiliary function $\psi(r, \theta, \varphi)$ is normalized, as are the spherical harmonics $Y_J^M(\theta, \varphi)$. Consequently, the radial function $R(r)$ in Eq. 2 is also normalized, i.e.,

$$\int_0^\infty |R(r)|^2 r^2 dr = 1. \quad (\text{S1})$$

For the Hamiltonian in Eq. (1), the radial wave function takes the form:

$$R(r) = \left(\frac{2Z}{na_0} \right)^{3/2} R_n^l \left(\frac{2Zr}{na_0} \right), \quad (\text{S2})$$

where

$$R_n^l(x) = \sqrt{\frac{(n-l-1)!}{2n(n+l)!}} x^l e^{-x/2} L_{n-l-1}^{2l+1}(x), \quad (\text{S3})$$

and $L_{n-l-1}^{2l+1}(x)$ denotes the associated Laguerre polynomial. In this work, the symbol Z in the above expressions is replaced by an effective nuclear charge \tilde{Z} , defined as follows:

$$\tilde{Z} = \frac{n}{n^*} Z^*, \quad (\text{S4})$$

where Z^* and n^* are effective values determined according to Slater’s rules [15]. This substitution accounts for electron shielding effects in multi-electron atoms, allowing the use of hydrogen-like wave functions with effective parameters.

In this work, l in Eq. S2 is set to 3 for the angular momentum of f electrons. Whether l should instead be J , L , or S from spin–orbit coupling remains unclear. Laguerre functions can be expressed via hypergeometric functions, but may diverge for half-integer parameters. As our analysis is insensitive to the radial distribution, we temporarily adopt $l = 3$. Since the physical meaning of the auxiliary function is not fully established, the validity of this choice requires further investigation.

EXAMPLE OF NdCl₃

As stated in the text, taking NdCl₃ as an example. The total angular momentum of Nd³⁺ is $J = 9/2$. To analyze its symmetry, we first consider rotational symmetry. The nine nearest-neighbor Cl[−] ions surrounding Nd³⁺ generate a crystal field with threefold rotational symmetry. Substituting $J = 9/2$ and $\kappa = 3$ into Eq. 7, we obtain:

$$|\psi\rangle = \left\{ \begin{aligned} &C_{\frac{9}{2}} \left| \frac{9}{2} \right\rangle + C_{\frac{3}{2}} \left| \frac{3}{2} \right\rangle + C_{-\frac{3}{2}} \left| -\frac{3}{2} \right\rangle + C_{-\frac{9}{2}} \left| -\frac{9}{2} \right\rangle \\ &C_{\pm\frac{7}{2}} \left| \pm\frac{7}{2} \right\rangle + C_{\pm\frac{1}{2}} \left| \pm\frac{1}{2} \right\rangle + C_{\mp\frac{5}{2}} \left| \mp\frac{5}{2} \right\rangle \end{aligned} \right. . \quad (\text{S5})$$

Second, we examine horizontal mirror symmetry to further characterize the system. The nine nearest-neighbor Cl[−] ions exhibit horizontal mirror symmetry. According to Eq. 8, since $\kappa = 3$ is odd, we have $I + C_3 = S_6 \xrightarrow{+\sigma_z} C_{6m}$. Imposing horizontal mirror symmetry transforms S_6 into C_{6m} . Consequently, the true eigenstates of NdCl₃ form a subset of Eq. S5, adopting sixfold symmetry as follows:

$$|\psi\rangle = \left\{ \begin{aligned} &C_{\pm\frac{9}{2}} \left| \pm\frac{9}{2} \right\rangle + C_{\mp\frac{3}{2}} \left| \mp\frac{3}{2} \right\rangle \\ &C_{\pm\frac{7}{2}} \left| \pm\frac{7}{2} \right\rangle + C_{\mp\frac{5}{2}} \left| \mp\frac{5}{2} \right\rangle \\ &\left| \pm\frac{1}{2} \right\rangle \end{aligned} \right. . \quad (\text{S6})$$

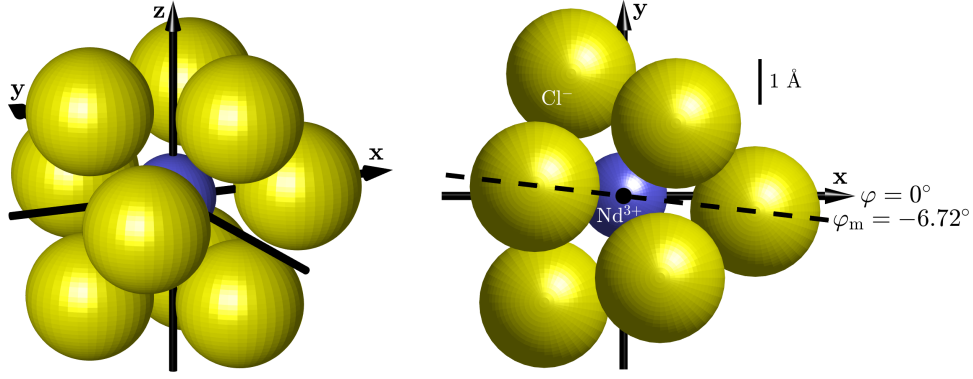


FIG. S1. The ionic structure of NdCl_3 . One of the vertical mirror is located at $\varphi_m = -6.72^\circ$.

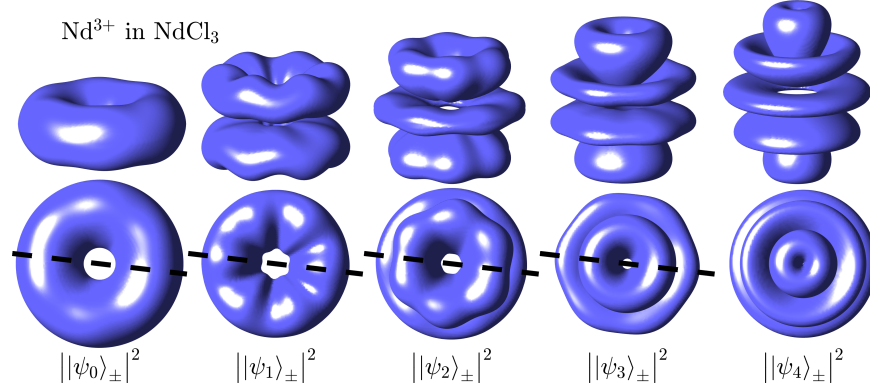


FIG. S2. Auxiliary densities of the eigenstates of NdCl_3 . They all satisfy the symmetries of the crystal field. The surface represents the equiprobability density surface that encloses 50% of the total auxiliary density.

For $|\pm \frac{1}{2}\rangle$, the difference in M with any other state is less than 6, with the maximum being 5. To realize sixfold rotational symmetry, $|\pm \frac{1}{2}\rangle$ must therefore remain isolated as a distinct state.

Third, we analyze the vertical mirror symmetry. As shown in Fig. S1, one of the vertical mirror planes of NdCl_3 is located at $\varphi_m = -6.72^\circ$. Using Eq. 9 and Eq. S6, we obtain:

$$\tan \text{Arg} \frac{C_{\pm \frac{9}{2}}}{C_{\mp \frac{3}{2}}} = \tan \text{Arg} \frac{C_{\pm \frac{7}{2}}}{C_{\mp \frac{5}{2}}} = \mp \tan(6\varphi_m) \approx \pm 0.849 \quad . \quad (\text{S7})$$

Using the auxiliary function, the results of Eq. S6 and Eq. S7 can be derived through straightforward analysis. These results are further validated by McPhase, a software package for computing static and dynamic magnetic properties of rare-earth compounds, including phase diagrams and excitations [35]. With McPhase, the precise ground and excited states of NdCl_3 can be obtained as follows:

$$\begin{cases} |\psi_0\rangle_{\pm} = 0.9989 |\pm \frac{9}{2}\rangle + (0.0359 \mp 0.0296i) |\mp \frac{3}{2}\rangle \\ |\psi_1\rangle_{\pm} = 0.9909 |\pm \frac{7}{2}\rangle + (0.1037 \mp 0.0855i) |\mp \frac{5}{2}\rangle \\ |\psi_2\rangle_{\pm} = (-0.1037 \mp 0.0855i) |\pm \frac{7}{2}\rangle + 0.9909 |\mp \frac{5}{2}\rangle \\ |\psi_3\rangle_{\pm} = (-0.0359 \mp 0.0296i) |\pm \frac{9}{2}\rangle + 0.9989 |\mp \frac{3}{2}\rangle \\ |\psi_4\rangle_{\pm} = |\pm \frac{1}{2}\rangle \end{cases} \quad . \quad (\text{S8})$$

It can be seen that all the eigenstates conform to Eq. S6, which verifies the validity of the result obtained by auxiliary function.

The coefficients in Eq. S8 can be calculated as follows:

$$\tan \text{Arg} \frac{C_{\pm \frac{9}{2}}}{C_{\mp \frac{3}{2}}} = \tan \text{Arg} \frac{C_{\pm \frac{7}{2}}}{C_{\mp \frac{5}{2}}} \approx \pm 0.824 \quad . \quad (\text{S9})$$

A comparison between Eq. S7 and Eq. S9 shows that the prediction in Eq. S7 is highly accurate, exhibiting only a very small discrepancy from Eq. S9, likely due to the approximations in the McPhase calculation.

We have plotted the auxiliary density distribution corresponding to the intrinsic states of NdCl_3 , as shown in Fig. S2. It is evident that the distribution perfectly conforms to the symmetry inherent in the crystal field.

ABOUT LEGENDRE FUNCTIONS

4 important properties

In this work, we need to find or construct a Legendre function $P_J^M(x)$ that satisfies the following four properties:

$$\left[(1-x^2) \frac{d^2}{dx^2} - 2x \frac{d}{dx} + J(J+1) - \frac{M^2}{1-x^2} \right] P_J^M(x) = 0, \quad (\text{S10})$$

$$\int_0^1 |P_J^M(x)|^2 dx = \frac{1}{2J+1} \frac{(J+M)!}{(J-M)!}, \quad (\text{S11})$$

$$\left| \frac{P_J^{-M}(x)}{(J-M)!} \right| = \left| \frac{P_J^M(x)}{(J+M)!} \right|, \quad (\text{S12})$$

$$P_J^M(x) = (-1)^{J+M} P_J^M(-x). \quad (\text{S13})$$

These four properties hold for associated Legendre polynomials with integer degree and order. For half-integer degrees, constructing the corresponding functions requires additional care. Properties (S10–S13) correspond one-to-one to those listed in Table I, with the second and third properties in the table weaker than those in Eqs. S11 and S12 to accommodate Hunter's alternative normalization convention.

Eq. S10–S13 each have specific implications for the spherical harmonics $Y_J^M(\theta, \varphi) = \sqrt{\frac{(2J+1)(J-M)!}{4\pi(J+M)!}} P_J^M(\cos \theta) e^{iM\varphi}$.

Equation S10 ensures that $Y_J^M(\theta, \varphi)$ is an eigenfunction of \hat{L}^2 with eigenvalue $J(J+1)\hbar^2$ and of \hat{L}_z with eigenvalue $M\hbar$, namely:

$$\hat{L}^2 Y_J^M(\theta, \varphi) = -\hbar^2 \left(\frac{1}{\sin \theta} \frac{\partial}{\partial \theta} \sin \theta \frac{\partial}{\partial \theta} + \frac{1}{\sin^2 \theta} \frac{\partial^2}{\partial \varphi^2} \right) Y_J^M(\theta, \varphi) = J(J+1)\hbar^2 Y_J^M(\theta, \varphi), \quad (\text{S14})$$

$$\hat{L}_z Y_J^M(\theta, \varphi) = \frac{\hbar}{i} \frac{\partial}{\partial \varphi} Y_J^M(\theta, \varphi) = M\hbar Y_J^M(\theta, \varphi). \quad (\text{S15})$$

Equation S11 ensures that Y_J^M satisfies the normalization condition, namely:

$$\int_0^{2\pi} \int_0^\pi |Y_J^M(\theta, \varphi)|^2 \sin \theta d\theta d\varphi = 1. \quad (\text{S16})$$

Equation S12 ensures that the auxiliary density distributions of $|-M\rangle$ and $|+M\rangle$ are identical, namely:

$$\frac{|\psi_J^{-M}(\theta, \varphi)|^2}{|\psi_J^M(\theta, \varphi)|^2} = \frac{|Y_J^{-M}(\theta, \varphi)|^2}{|Y_J^M(\theta, \varphi)|^2} = 1. \quad (\text{S17})$$

Equation S13 ensures that the auxiliary density of any superposition state exhibits inversion symmetry, namely:

$$|\psi(\theta, \varphi)|^2 = |\psi(\pi - \theta, \varphi + \pi)|^2. \quad (\text{S18})$$

This is crucial for the symmetry analysis presented in this work and is proved in detail in a later section.

Two important approaches exist for extending the associated Legendre polynomials to non-integer orders and degrees. The more widely used method is due to Hobson [20, 21], while the other was proposed by Hunter *et al.* [29, 30].

TABLE S1. Hobson's $P_J^M(x)$.

$M \downarrow$	$J = \frac{1}{2}$	$J = \frac{3}{2}$	$J = \frac{5}{2}$	$J = \frac{7}{2}$	$J = \frac{9}{2}$
$\frac{9}{2}$					$\frac{3x(128x^8 - 576x^6 + 1008x^4 - 840x^2 + 315)}{\sqrt{\frac{\pi}{2}\sqrt{(1-x^2)^9}}}$
$\frac{7}{2}$				$\frac{3x(16x^6 - 56x^4 + 70x^2 - 35)}{\sqrt{\frac{\pi}{2}\sqrt{(1-x^2)^7}}}$	$\frac{3(128x^8 - 448x^6 + 560x^4 - 280x^2 + 35)}{\sqrt{\frac{\pi}{2}\sqrt{(1-x^2)^7}}}$
$\frac{5}{2}$			$\frac{x(8x^4 - 20x^2 + 15)}{\sqrt{\frac{\pi}{2}\sqrt{(1-x^2)^5}}}$	$\frac{3(16x^6 - 40x^4 + 30x^2 - 5)}{\sqrt{\frac{\pi}{2}\sqrt{(1-x^2)^5}}}$	$\frac{3x(64x^6 - 168x^4 + 140x^2 - 35)}{\sqrt{\frac{\pi}{2}\sqrt{(1-x^2)^5}}}$
$\frac{3}{2}$		$\frac{x(2x^2 - 3)}{\sqrt{\frac{\pi}{2}\sqrt{(1-x^2)^3}}}$	$\frac{8x^4 - 12x^2 + 3}{\sqrt{\frac{\pi}{2}\sqrt{(1-x^2)^3}}}$	$\frac{x(24x^4 - 40x^2 + 15)}{\sqrt{\frac{\pi}{2}\sqrt{(1-x^2)^3}}}$	$\frac{64x^6 - 120x^4 + 60x^2 - 5}{\sqrt{\frac{\pi}{2}\sqrt{(1-x^2)^3}}}$
$\frac{1}{2}$	$\frac{x}{\sqrt{\frac{\pi}{2}\sqrt{1-x^2}}}$	$\frac{2x^2 - 1}{\sqrt{\frac{\pi}{2}\sqrt{1-x^2}}}$	$\frac{x(4x^2 - 3)}{\sqrt{\frac{\pi}{2}\sqrt{1-x^2}}}$	$\frac{8x^4 - 8x^2 + 1}{\sqrt{\frac{\pi}{2}\sqrt{1-x^2}}}$	$\frac{x(16x^4 - 20x^2 + 5)}{\sqrt{\frac{\pi}{2}\sqrt{1-x^2}}}$
$-\frac{1}{2}$	$\sqrt{\frac{2}{\pi}}\sqrt{1-x^2}$	$x\sqrt{\frac{2}{\pi}}\sqrt{1-x^2}$	$\frac{1}{3}(4x^2 - 1)\sqrt{\frac{2}{\pi}}\sqrt{1-x^2}$	$x(2x^2 - 1)\sqrt{\frac{2}{\pi}}\sqrt{1-x^2}$	$\frac{1}{5}(16x^4 - 12x^2 + 1)\sqrt{\frac{2}{\pi}}\sqrt{1-x^2}$
$-\frac{3}{2}$		$\frac{1}{3}\sqrt{\frac{2}{\pi}}(1-x^2)^{\frac{3}{4}}$	$\frac{x}{3}\sqrt{\frac{2}{\pi}}(1-x^2)^{\frac{3}{4}}$	$\frac{1}{15}(6x^2 - 1)\sqrt{\frac{2}{\pi}}(1-x^2)^{\frac{3}{4}}$	$\frac{x}{15}(8x^2 - 3)\sqrt{\frac{2}{\pi}}(1-x^2)^{\frac{3}{4}}$
$-\frac{5}{2}$			$\frac{1}{15}\sqrt{\frac{2}{\pi}}(1-x^2)^{\frac{5}{4}}$	$\frac{x}{15}\sqrt{\frac{2}{\pi}}(1-x^2)^{\frac{5}{4}}$	$\frac{1}{105}(8x^2 - 1)\sqrt{\frac{2}{\pi}}(1-x^2)^{\frac{5}{4}}$
$-\frac{7}{2}$				$\frac{1}{105}\sqrt{\frac{2}{\pi}}(1-x^2)^{\frac{7}{4}}$	$\frac{x}{105}\sqrt{\frac{2}{\pi}}(1-x^2)^{\frac{7}{4}}$
$-\frac{9}{2}$					$\frac{1}{945}\sqrt{\frac{2}{\pi}}(1-x^2)^{\frac{9}{4}}$

Hobson's Legendre function

Hobson's Legendre functions, obtained by solving the associated Legendre equation with complex parameters, come in two types: $P_\lambda^\mu(z)$ and $Q_\lambda^\mu(z)$. Among these, $P_\lambda^\mu(z)$ serves as the natural extension of the Legendre polynomial, with its explicit form given by [20–28]:

$$P_\lambda^\mu(z) = \frac{1}{(-\mu)!} \left(\frac{z+1}{z-1} \right)^{\mu/2} {}_2F_1 \left(-\lambda, \lambda+1; 1-\mu; \frac{1-z}{2} \right), \quad (\text{S19})$$

where λ , μ , and z may be complex, and ${}_2F_1$ denotes the hypergeometric function. When λ and μ are integers or half-integers J and M , the standard Legendre function $P_J^M(x)$ can be expressed as follows:

$$P_J^M(x) = \frac{(J+M)!}{(J-M)!} \frac{(1-x^2)^{-M/2}}{2^J} \sum_{k=0}^{[(J+M)/2]} \frac{(-1)^k (2J-2k)!}{k! (J-k)!} \frac{x^{J+M-2k}}{(J+M-2k)!}. \quad (\text{S20})$$

This result can also be derived from the generalized Rodrigues formula of the associated Legendre function, as follows:

$$P_J^M(x) = \frac{(-1)^M}{2^J J!} (1-x^2)^{M/2} \frac{d^{J+M}}{dx^{J+M}} (x^2-1)^J. \quad (\text{S21})$$

These results agree with those given in Eqs. S19 and S20. Table S1 presents specific forms of Hobson's $P_J^M(x)$.

The associated Legendre polynomials arise as the special case of Eq. S19 with $\lambda \in \mathbb{N}$ and $\mu \in [-\lambda, \lambda] \cap \mathbb{Z}$. In this case, the prefactor $(-\lambda)$ in Eq. S19 forces all terms with indices greater than λ to vanish, truncating the infinite series to a finite sum. Consequently, the Legendre function reduces to polynomials.

Hobson's Legendre functions satisfy Eq. S10 and Eq. S13, but for half-integer degrees and orders they do not satisfy Eq. S12. For half-integer orders $M < 1$, Eq. S11 remains valid; for half-integer orders $M > 1$, however, Eq. S11 breaks down and the integral diverges. Hence, no normalization coefficient can be defined, and the functions are intrinsically non-normalizable.

Since Hobson's Legendre functions fail to satisfy Eq. S11 and Eq. S12, they are not suitable for the present work.

Hunter's Legendre function

Hunter *et al.* proposed an alternative formulation of Legendre function parameters, valid when both the degree and the order are integers or half-integers [29, 30]. By carefully examining the associated Legendre polynomials, patterns

TABLE S2. Hunter's $P_J^M(x)$: In Hunter's convention, $P_J^M(x)$ may be taken as $P_J^{|M|}(x)$ for $M < 0$.

$M \downarrow$	$J = \frac{1}{2}$	$J = \frac{3}{2}$	$J = \frac{5}{2}$	$J = \frac{7}{2}$	$J = \frac{9}{2}$
$\frac{9}{2}$					$(1-x^2)^{\frac{9}{4}}$
$\frac{7}{2}$				$(1-x^2)^{\frac{7}{4}}$	$x(1-x^2)^{\frac{7}{4}}$
$\frac{5}{2}$			$(1-x^2)^{\frac{5}{4}}$	$x(1-x^2)^{\frac{5}{4}}$	$(1-8x^2)(1-x^2)^{\frac{5}{4}}$
$\frac{3}{2}$		$(1-x^2)^{\frac{3}{4}}$	$x(1-x^2)^{\frac{3}{4}}$	$(1-6x^2)(1-x^2)^{\frac{3}{4}}$	$x(3-8x^2)(1-x^2)^{\frac{3}{4}}$
$\frac{1}{2}$	$\sqrt[4]{1-x^2}$	$x\sqrt[4]{1-x^2}$	$(1-4x^2)\sqrt[4]{1-x^2}$	$3x(1-2x^2)\sqrt[4]{1-x^2}$	$3(16x^4-12x^2+1)\sqrt[4]{1-x^2}$

among the factors can be identified and extended to half-integer parameters. Hunter also provided a table of these factors [29], from which Table S2 lists expressions of several Hunter's Legendre functions.

Hunter's results are expressed entirely as polynomials and are valid only when both the degree and the order are integers or half-integers, and they do not extend to general fractional parameters. Strictly speaking, these should be called Hunter's Legendre polynomials, but for simplicity we refer to them here as Hunter's Legendre functions.

Hunter provided expressions for P_J^M only for $M \geq 0$, since $M < 0$ is unnecessary: according to Hunter's convention, the spherical harmonics are defined as $Y_J^M \equiv P_J^{|M|}(\cos \theta)e^{iM\varphi}$ [30], making $P_J^{-|M|}$ redundant. Equivalently, one can understand this as defining $P_J^{-|M|} \equiv P_J^{|M|}$. It is under this understanding that the third condition in Table I is marked with a \checkmark . Furthermore, it is straightforward to verify that the squared modulus of these polynomials is integrable, so the second condition in Table I is also satisfied.

Although Hunter's functions do not strictly satisfy Eqs. S11 and S12, this discrepancy arises only from differences in coefficient definitions; they still satisfy the integrability and symmetry implied by these equations. Hunter correctly identified the underlying patterns, and his functions do satisfy the associated Legendre equation (Eq. S10). Therefore, Hunter's Legendre functions meet three of the four conditions, but they do not satisfy the fourth condition in Table I (Eq. S13). If the auxiliary function is chosen as Hunter's Legendre function, the resulting auxiliary density may fail to preserve inversion symmetry in certain cases—specifically, when J is half-integer and the superposition state includes both $M < 0$ and $M > 0$ components. Consequently, Hunter's approach is also not ideal, and a new formulation of Legendre functions remains necessary.

Legendre function in this work

None of the existing approaches is fully satisfactory, motivating an alternative design that satisfies all four conditions: Eqs. S10–S13. Hobson's Legendre functions fail to satisfy Eqs. S11 and S12, while Hunter's functions do not satisfy Eq. S13. For half-integer J and M , the third and fourth conditions are partially contradictory. For example, with $M = \pm 1/2$, Eq. S13 requires $P_J^{1/2}(x)$ and $P_J^{-1/2}(x)$ to have opposite parity, whereas Eq. S12 requires them to have the same parity. Constructing a Legendre function that satisfies both conditions is therefore nontrivial. This conflict is resolved by introducing the sign function $\text{sgn}(x)$, which allows simultaneous satisfaction of all four conditions.

Since it is generally impossible to satisfy Eqs. S10–S13 simultaneously, we must sacrifice continuity at $x = 0$. This is achieved by introducing a $\text{sgn}(x)$ factor. The Legendre function in this work is defined as follows:

$$P_\lambda^\mu(x)_{\text{this work}} \equiv (-1)^{(\mu+|\mu|)[\frac{1}{2}+2\lambda+\lambda \text{sgn}(x)]} \frac{(\lambda+\mu)!}{(\lambda-|\mu|)!} P_\lambda^{-|\mu|}(x)_{\text{Hobson}}, \quad (\text{S22})$$

where $\nu, \mu \in \mathbb{Z}$. For $2J \in \mathbb{N}$ and $M \in \{-J, 1-J, \dots, J\}$, Eq. 4 holds. Table S3 lists some $P_J^M(x)$ in this work for half-integer J and M at $x \neq 0$.

Introducing $\text{sgn}(x)$ changes the parity for positive half-integer M , converting odd functions into even ones and vice versa. This may produce a discontinuity at $x = 0$ when $J - M$ is even, but the auxiliary density often remains continuous in non-superposed states or when it possesses even-fold rotational symmetry.

As noted in the main text, the choice of the exponent of (-1) in Eq. S22 is not unique. We adopt $[\frac{1}{2}+2\lambda+\lambda \text{sgn}(x)]$

TABLE S3. $P_J^M(x)$ in this work for $x = \pm|x|$, with $x \neq 0$.

$M \downarrow$	$J = \frac{1}{2}$	$J = \frac{3}{2}$	$J = \frac{5}{2}$	$J = \frac{7}{2}$	$J = \frac{9}{2}$
$\frac{9}{2}$					$\pm 384 \sqrt{\frac{2}{\pi}} (1-x^2)^{\frac{9}{4}}$
$\frac{7}{2}$				$\mp 48 \sqrt{\frac{2}{\pi}} (1-x^2)^{\frac{7}{4}}$	$\pm 384x \sqrt{\frac{2}{\pi}} (1-x^2)^{\frac{7}{4}}$
$\frac{5}{2}$			$\pm 8 \sqrt{\frac{2}{\pi}} (1-x^2)^{\frac{5}{4}}$	$\mp 48x \sqrt{\frac{2}{\pi}} (1-x^2)^{\frac{5}{4}}$	$\pm 24 (8x^2 - 1) \sqrt{\frac{2}{\pi}} (1-x^2)^{\frac{5}{4}}$
$\frac{3}{2}$		$\mp 2 \sqrt{\frac{2}{\pi}} (1-x^2)^{\frac{3}{4}}$	$\pm 8x \sqrt{\frac{2}{\pi}} (1-x^2)^{\frac{3}{4}}$	$\mp 4 (6x^2 - 1) \sqrt{\frac{2}{\pi}} (1-x^2)^{\frac{3}{4}}$	$\pm 8x (8x^2 - 3) \sqrt{\frac{2}{\pi}} (1-x^2)^{\frac{3}{4}}$
$\frac{1}{2}$	$\pm \sqrt{\frac{2}{\pi}} \sqrt{1-x^2}$	$\mp 2x \sqrt{\frac{2}{\pi}} \sqrt{1-x^2}$	$\pm (4x^2 - 1) \sqrt{\frac{2}{\pi}} \sqrt{1-x^2}$	$\mp 4x (2x^2 - 1) \sqrt{\frac{2}{\pi}} \sqrt{1-x^2}$	$\pm (16x^4 - 12x^2 + 1) \sqrt{\frac{2}{\pi}} \sqrt{1-x^2}$
$-\frac{1}{2}$	$\sqrt{\frac{2}{\pi}} \sqrt{1-x^2}$	$x \sqrt{\frac{2}{\pi}} \sqrt{1-x^2}$	$\frac{1}{3} (4x^2 - 1) \sqrt{\frac{2}{\pi}} \sqrt{1-x^2}$	$x (2x^2 - 1) \sqrt{\frac{2}{\pi}} \sqrt{1-x^2}$	$\frac{1}{5} (16x^4 - 12x^2 + 1) \sqrt{\frac{2}{\pi}} \sqrt{1-x^2}$
$-\frac{3}{2}$		$\frac{1}{3} \sqrt{\frac{2}{\pi}} (1-x^2)^{\frac{3}{4}}$	$\frac{x}{3} \sqrt{\frac{2}{\pi}} (1-x^2)^{\frac{3}{4}}$	$\frac{1}{15} (6x^2 - 1) \sqrt{\frac{2}{\pi}} (1-x^2)^{\frac{3}{4}}$	$\frac{x}{15} (8x^2 - 3) \sqrt{\frac{2}{\pi}} (1-x^2)^{\frac{3}{4}}$
$-\frac{5}{2}$			$\frac{1}{15} \sqrt{\frac{2}{\pi}} (1-x^2)^{\frac{5}{4}}$	$\frac{x}{15} \sqrt{\frac{2}{\pi}} (1-x^2)^{\frac{5}{4}}$	$\frac{1}{105} (8x^2 - 1) \sqrt{\frac{2}{\pi}} (1-x^2)^{\frac{5}{4}}$
$-\frac{7}{2}$				$\frac{1}{105} \sqrt{\frac{2}{\pi}} (1-x^2)^{\frac{7}{4}}$	$\frac{x}{105} \sqrt{\frac{2}{\pi}} (1-x^2)^{\frac{7}{4}}$
$-\frac{9}{2}$					$\frac{1}{945} \sqrt{\frac{2}{\pi}} (1-x^2)^{\frac{9}{4}}$

to ensure that the function near $x = 0$ has the same sign as Hobson's Legendre function, i.e.,

$$\lim_{\delta \rightarrow 0} \text{sgn} \left(\frac{P_J^M(\pm\delta)_{\text{This work}}}{P_J^M(\pm\delta)_{\text{Hobson}}} \right) = 1.$$

The explicit $\text{sgn}(x)$ factor, absent in prior literature, makes our Legendre function a fundamentally new and practical tool. It applies to both half-integer and integer cases and provides valuable insights into symmetry properties.

PROOF OF INVERSION SYMMETRY IN THE AUXILIARY DENSITY

The auxiliary density $|\psi|^2$ of a superposition is always inversion-symmetric. Equation S13 plays a crucial role in this property. We will use it to prove the inversion symmetry of the auxiliary density in this section.

For a single auxiliary function, the auxiliary density is:

$$|\psi(r, \theta, \varphi)|^2 = |A(r)P_J^M(\cos\theta)e^{iM\varphi}|^2 \quad (\text{S23})$$

For cases in which J and M are both integers or half-integers (as below), with Eq. S13, the auxiliary density at the inversion position can be derived using Eq. S13 as follows:

$$|\psi(r, \pi - \theta, \varphi + \pi)|^2 = |A(r)P_J^M(-\cos\theta)(-e^{iM\varphi})|^2 = |A(r)P_J^M(\cos\theta)e^{iM\varphi}|^2 = |\psi(r, \theta, \varphi)|^2. \quad (\text{S24})$$

Thus, the inversion symmetry of singlet auxiliary density is proved.

Consider the superposition of two states $|\psi\rangle = |C_1| M_1\rangle + |C_2| M_2\rangle$, the auxiliary density is:

$$\begin{aligned}
& |\psi(r, \theta, \varphi)|^2 \\
&= |C_1 | M_1\rangle + C_2 | M_2\rangle|^2 \\
&= \left| A(r)P_J^{M_1}(\cos\theta)e^{iM_1\varphi} + B(r)P_J^{M_2}(\cos\theta)e^{iM_2\varphi} \right|^2 \\
&= \left| AP_J^{M_1}(\cos\theta) \right|^2 + \left| BP_J^{M_2}(\cos\theta) \right|^2 \\
&\quad + 2 \left| ABP_J^{M_1}(\cos\theta)P_J^{M_2}(\cos\theta) \right| \cos \left\{ (M_1 - M_2)\varphi + \text{Arg} \left[AP_J^{M_1}(\cos\theta)B^*P_J^{M_2}(\cos\theta)^* \right] \right\} \\
&= \left| AP_J^{M_1}(\cos\theta) \right|^2 + \left| BP_J^{M_2}(\cos\theta) \right|^2 \\
&\quad + 2 \left| ABP_J^{M_1}(\cos\theta)P_J^{M_2}(\cos\theta) \right| \cos \left\{ (M_1 - M_2)\varphi + \text{Arg} (AB^*) + \text{Arg} \left[P_J^{M_1}(\cos\theta)P_J^{M_2}(\cos\theta) \right] \right\}. \quad (\text{S25})
\end{aligned}$$

Here, A and B depend only on r and are independent of θ and φ . The auxiliary density at the inversion position is:

$$\begin{aligned} & |\psi(r, \pi - \theta, \varphi + \pi)|^2 \\ &= \left| AP_J^{M_1}(-\cos\theta) \right|^2 + \left| BP_J^{M_2}(-\cos\theta) \right|^2 \\ &\quad + 2 \left| ABP_J^{M_1}(-\cos\theta)P_J^{M_2}(-\cos\theta) \right| \cos \left\{ (M_1 - M_2)(\varphi + \pi) + \text{Arg}(AB^*) + \text{Arg} \left[P_J^{M_1}(-\cos\theta)P_J^{M_2}(-\cos\theta) \right] \right\} \quad (\text{S26}) \end{aligned}$$

$$\begin{aligned} &= \left| AP_J^{M_1}(\cos\theta) \right|^2 + \left| BP_J^{M_2}(\cos\theta) \right|^2 \\ &\quad + 2 \left| ABP_J^{M_1}(\cos\theta)P_J^{M_2}(\cos\theta) \right| \cos \left\{ (M_1 - M_2)(\varphi + \pi) + \text{Arg}(AB^*) + \text{Arg} \left[(-1)^{J+M_1}P_J^{M_1}(\cos\theta) \cdot (-1)^{J+M_2}P_J^{M_2}(\cos\theta) \right] \right\} \quad (\text{S27}) \end{aligned}$$

$$\begin{aligned} &= \left| AP_J^{M_1}(\cos\theta) \right|^2 + \left| BP_J^{M_2}(\cos\theta) \right|^2 + 2 \left| ABP_J^{M_1}(\cos\theta)P_J^{M_2}(\cos\theta) \right| \\ &\quad \cdot \cos \left\{ (M_1 - M_2)\varphi + \text{Arg}(AB^*) + \text{Arg} \left[P_J^{M_1}(\cos\theta)P_J^{M_2}(\cos\theta) \right] + (M_1 - M_2)\pi + \text{Arg} \left[(-1)^{2J+M_1+M_2} \right] \right\} \\ &= \left| AP_J^{M_1}(\cos\theta) \right|^2 + \left| BP_J^{M_2}(\cos\theta) \right|^2 + 2 \left| ABP_J^{M_1}(\cos\theta)P_J^{M_2}(\cos\theta) \right| \\ &\quad \cdot \cos \left\{ (M_1 - M_2)\varphi + \text{Arg}(AB^*) + \text{Arg} \left[P_J^{M_1}(\cos\theta)P_J^{M_2}(\cos\theta) \right] + (M_1 - M_2)\pi + (2J + M_1 + M_2)\pi \right\} \\ &= \left| AP_J^{M_1}(\cos\theta) \right|^2 + \left| BP_J^{M_2}(\cos\theta) \right|^2 \\ &\quad + 2 \left| ABP_J^{M_1}(\cos\theta)P_J^{M_2}(\cos\theta) \right| \cos \left\{ (M_1 - M_2)\varphi + \text{Arg}(AB^*) + \text{Arg} \left[P_J^{M_1}(\cos\theta)P_J^{M_2}(\cos\theta) \right] + 2\pi(J + M_1) \right\} \\ &= \left| AP_J^{M_1}(\cos\theta) \right|^2 + \left| BP_J^{M_2}(\cos\theta) \right|^2 \\ &\quad + 2 \left| ABP_J^{M_1}(\cos\theta)P_J^{M_2}(\cos\theta) \right| \cos \left\{ (M_1 - M_2)\varphi + \text{Arg}(AB^*) + \text{Arg} \left[P_J^{M_1}(\cos\theta)P_J^{M_2}(\cos\theta) \right] \right\} \quad (\text{S28}) \\ &= |\psi(r, \theta, \varphi)|^2. \end{aligned}$$

This completes the proof. It is worth noting that the transition from Eq. S26 to Eq. S27 relies directly on Eq. S13. For superpositions involving more than two states, the proof follows the same reasoning and is omitted here.

Strictly speaking, Eq. S13 is not a necessary and sufficient condition. A weaker requirement that still ensures inversion symmetry of a superposition is:

$$\frac{P_J^{M+1}(-x)}{P_J^{M+1}(x)} = -\frac{P_J^M(-x)}{P_J^M(x)}. \quad (\text{S29})$$

Hunter's Legendre functions do not satisfy Eq. S29 for $M = -\frac{1}{2}$. With these functions, the corresponding density retains inversion symmetry only when all M values in the superposition share the same sign; once both positive and negative M appear, the symmetry is lost. Hence, Hunter's functions are not applicable in this context, and our conclusions remain unaffected.

We have thus demonstrated that, for both single states and superpositions, and for angular momenta that are either integer or half-integer, the auxiliary density universally exhibits inversion symmetry:

$$|\psi(r, \theta, \varphi)|^2 = |\psi(r, \pi - \theta, \varphi + \pi)|^2. \quad (\text{S30})$$